

ENGINEERING RESEARCH INSTITUTE  
THE UNIVERSITY OF MICHIGAN  
ANN ARBOR

Final Report

VARIATIONS IN SPECTRAL SENSITIVITY WITHIN THE HUMAN FOVEA

H. Richard Blackwell  
J. H. Taylor

Vision Research Laboratories

ERI Project 2455

BUREAU OF SHIPS, DEPARTMENT OF THE NAVY  
CONTRACT NO. Nobs-72038  
WASHINGTON, D. C.

June 1958

ensm

UMR0443

2455-10-F

The experiments reported here represent the basis for the  
doctoral dissertation:

"Variations in Spectral Sensitivity

Within the Human Fovea"

by

John Hall Taylor

University of Michigan, 1952

2455-10-F

TABLE OF CONTENTS

	<u>Title</u>	<u>Page</u>
	List of Figures	iii
	List of Tables	iv
	Summary	v
I.	Introduction	1
II.	Procedures and Apparatus	6
III.	Results and Discussion	15
	References	19

2455-10-F

LIST OF FIGURES

<u>Number</u>	<u>Title</u>
1	Spectral sensitivity data of Hsia and Graham (1952)
2	Spectral Sensitivity data of Crozier (1950)
3	Schematic diagram of optical apparatus
4	Diagram of thermopile circuitry
5	Measurements of ocular chromatic aberration
6	Spectral sensitivity data for NLT: zero eccentricity
7	Spectral sensitivity data for NLT: 15 minutes eccentricity
8	Spectral sensitivity data for NLT: 43 minutes eccentricity
9	Spectral sensitivity data for JHT: zero eccentricity
10	Spectral sensitivity data for JHT: 15 minutes eccentricity
11	Spectral sensitivity data for JHT: 43 minutes eccentricity
12	Spectral sensitivity data for DWM: zero eccentricity
13	Spectral sensitivity data for DWM: 15 minutes eccentricity
14	Spectral sensitivity data for DWM: 43 minutes eccentricity
15	Spectral sensitivity data for NLT: all eccentricities
16	Spectral sensitivity data for JHT: all eccentricities
17	Spectral sensitivity data for DWM: all eccentricities

2455-10-F

LIST OF TABLES

- I Summary of Radiometric Measurements and Their Conversion to Units of Energy at the Cornea
- II Residual Errors after Correction for Chromatic Aberration (diopters)
- III Spectral Sensitivity for Observer NLT; Inverse Threshold Radiosity (microwatts x  $10^{-6}$ )
- IV Spectral Sensitivity for Observer JHT; Inverse Threshold Radiosity (microwatts x  $10^{-6}$ )
- V Spectral Sensitivity for Observer DWM; Inverse Threshold Radiosity (microwatts x  $10^{-6}$ )

2455-10-F

SUMMARY

Spectral sensitivity curves have been measured at each of three foveal locations in each of three human eyes, utilizing a circular target subtending 1 minute of arc. Target exposure duration was 0.1 second; an artificial pupil of 6.04 mm. diameter was used. The temporal forced-choice variant of the method of constant stimuli was employed, utilizing automatic presentation and recording equipment. A total of 24,750 observations were made in all. Precautions were taken to insure that the various chromatic targets would be as well focused as possible, by the use of matching chromatic fixation lights, and by measurements of the chromatic aberration of the eye and the use of ophthalmic corrections to compensate.

Spectral sensitivity was found to vary in an idiosyncratic manner from location to location and from eye to eye, to an extent far in excess of experimental uncertainties. The sensitivity curves were generally irregular, often exhibiting two peaks. In different curves, peaks were found at about 460, 480, 510, 525, 540, 555, and 610  $\mu$ . These data suggest that a large number of cone types may exist and that sensitivity for small retinal areas may represent the action of various combinations of the various classes of cones.

The spectral sensitivity data were related to the various areas which are differentiated in the entoptic image of the macula reported by the three observers. It was found that differences in sensitivity over the blue end of the spectrum were predicted very adequately by differences in the macular entoptic image. Since tritanopia does not have an appreciable effect upon the spectral sensitivity curves, these data suggest that the entoptic image of the macula is produced by differences in the density of the macular pigment.

## I. INTRODUCTION

The spectral sensitivity of the eye has been studied by many investigators, under a wide variety of conditions. These investigations have revealed the existence of photoreceptors with two markedly different spectral sensitivity curves. One spectral sensitivity curve has a maximum at about 505 m $\mu$  and is associated with the rod photoreceptors which are distributed throughout the entire retina except for the fovea. The other spectral sensitivity curve has a maximum at about 555 m $\mu$  and is associated with the cone photoreceptors which are distributed throughout the entire retina with heavy concentration in the rod-free fovea.

Among the most recent measurements of the spectral sensitivity of the foveal cone photoreceptors are those of Hsia and Graham (Ref. 1), which are presented in Figure 1. The test target used for these measurements subtended 42 minutes of arc. The principle peak of the curve is at 550 m $\mu$ , with marked secondary peaks at about 440 m $\mu$  and about 620 m $\mu$ . The curve presented in Figure 1 represents the average of the data for five observers. The general smoothness of the tri-modal function is apparent. Of course, averaging data in this way tends to smooth out small irregularities. However, the data for the individual observers in the Hsia and Graham study are generally smooth so that the average curve seems to be an adequate representation of all the data.

More recent data by Sperling (Ref. 2) demonstrate that the spectral sensitivity curve of the human fovea depends to some extent upon the angular size of the test target. In general, the curve exhibits more irregularity as the size of the test target is reduced from 42. to 3. minutes of arc.

The spectral sensitivity of the human fovea has been measured for test targets of essentially point-size by Crozier (Ref. 3). The test target was a square, subtending 1.6 minutes on a side; the exposure duration varied between 0.051 and 0.0785 seconds. These data are presented in Figure 2, the scales being identical with those used in Figure 1. There appear to be a number of peaks in this curve and its general form is quite different from the curve representing the Hsia and Graham data obtained with the larger test target.

The dependence of the form of the spectral sensitivity function upon target size illustrated by a comparison of Figures 1 and 2 has considerable practical and theoretical significance. Luminous signals used in military operations are frequently viewed at such long distances that their subtense is essential point-size. In assessing the design and use of these signals, account must be taken of the effect of target size upon the spectral sensitivity curve.



The dependence of spectral sensitivity upon target size is of theoretical interest because of its relation to anatomical and physiological properties of various portions of the human fovea. These properties of the eye will be discussed in the following sections.

Morphologically, the fovea comprises a roughly circular area at the retinal center with a diameter of about 1.5 mm., which thus subtends about 5 degrees of arc. The fovea is seen as a depression on the vitreal surface of the retina, and if the area is examined microscopically in cross section, it is apparent that certain of the tissue layers present elsewhere in the retina (Polyak's layers 5 to 9) are here absent or attenuated. The outer nuclear and bacillary layers are somewhat thickened, and it has been shown that as the center is approached there are progressively fewer rods and more cones until in the centermost 0.5 mm., only cones are present. This rod-free area subtends 100 minutes according to the recent results of Polyak (Ref. 4).

#### The Macula Lutea

Buzzi (Ref. 5), who first reported the existence of the fovea, noted the presence of a yellow pigment which permeates certain of the tissues in the region of the central retina. This area of the retina, known as the macula lutea, or yellow spot, has a maximal diameter of 5 mm. or more in man, although the pigmentation is only faintly observable in the outer 1 mm. band and it seems likely that 3 mm. is the effective limit, corresponding to 10 degrees of visual angle. The densest pigment occurs on the slopes and margin of the inner fovea, while on the floor of the foveal pit where the tissues that elsewhere carry the pigment are extremely thin and the non-pigmented photoreceptor layers are thickened, there is an area about 0.4 mm. across (80. minutes) which is relatively free of pigment. In the opinion of Polyak (op. cit.) the pigment is present in the living eye, and is not, as was claimed by Gullstrand (Ref. 6) and others, a postmortem phenomenon.

Because the macular pigment is present in those layers of the retina which overlie the layer of rods and cones (Polyak's layers 4 to 10) it has long been recognized that its effect in vision must be that of a yellow filter intercepting the light reaching the macular area. The usual consequence of interposing a yellow filter in this manner is reduction of luminosity of the short-wave components of the incident light; thus, white light appears yellow; red, yellow, and green are relatively unchanged; and blue is partly or wholly absorbed. In our usual visual experience, however, we are never aware of a yellow annulus in the visual field, and it must be assumed that sensory constancy, perhaps coupled with local adaptation at the retinal or higher neural levels, operates to maintain apparent uniformity of the field. Only under certain special conditions of viewing can the macula lutea be observed entoptically and its configuration in

the living eye estimated.

Entoptic Observation of the Macula

A technique for making the macular pigment appear in an entoptic image was first described by Maxwell (Ref. 7), who recommended that pieces of blue and yellow glass be alternated before the eye while regarding a uniformly lit surface. At appropriate rates of alternation, a dark spot appears in the blue phase and disappears in the yellow, the whole experience being exceedingly transient. Helmholtz (Ref. 8) ascribed the dark spot to differential rates of adaptation of the cones depending upon density of the overlying pigment. More recently Miles (Ref. 9) has proposed a method whereby most individuals can observe and plot the extent and character of their own maculae. His technique consists in the fixation of a small point on a uniformly white surface while two filter, dichroic purple and a neutral of corresponding visual density, are alternated in front of the eye. This procedure results in an entoptic image whose outline and texture may be sketched by the observer.

The most commonly reported entoptic macular image by Miles' procedure has the following features:

1. A central dark spot with well-defined edges. The average angular subtense, as determined from 26 single eyes, is 32 minutes.
2. A clear annular band which appears relatively bright and has an average outside diameter of 70 minutes. The outer edge of this area is quite well-defined.
3. A broad ring lying outside the clear area, appearing to have about the same brightness as the central dark spot. The average value for the overall diameter of this area is 160 minutes. The outer edge of this area is quite variable between observers, appearing smooth, asteroid, scalloped, or like a "shell burst" to various observers.

The magnitude of the elements of the macular image do not, in some respects, correspond with the histological data. The outermost dark area in the macular image subtends an average of 160 minutes instead of the 5 degrees believed to be the angular diameter of the entire foveal excavation. The 160 minute dimension does however correspond well with the zone of greatest pigment density. The bright annular band has outer dimensions which agree with the outer dimensions of the floor of the foveal excavation. The floor of the foveal excavation (nonpigmented) subtends 80 minutes, whereas the annular area was found to have an average outer diameter of 70 minutes. The central dark area of the macular images is of doubtful origin. No evidence exists from tissue studies that there is a spot of pigment in the very center of the foveal excavation which would correspond to this area. There is, however, a region of the foveal excavation which is still further indented, called the umbo. The diameter of the umbo has not been definitely determined, but it seems reasonable to suppose that, since the umbo is probably the

retinal fixation point, it may correspond closely to the dark central area of the macular figure. Two anatomical possibilities then exist: either the umbo contains some yellow pigment as yet undiscovered histologically, or the sharply inclined walls of the umbo result in some refractive phenomenon which acts in the same manner as does the macular pigment.

#### Physical Measurement of the Macular Pigment

A more direct assessment of the yellow pigment has been attempted by Wald (Ref. 10), who has presented spectrophotometric curves for a crude extract of human maculae. The absorption spectrum so obtained is, as Wald points out, virtually identical with that of crystalline leaf xanthophyll, maximal absorption occurring in the neighborhood of 460 m $\mu$ . In addition to these curves, Wald presents some visual estimates of pigment density which show wide individual differences between observers; some apparently having no pigment whatever, and others having sufficient pigment density so that as much as 90 per cent of the light is absorbed at 436 m $\mu$ .

#### Dichromasy of the Central Fovea

In 1894 Konig (Ref. 11) reported the hitherto unnoticed fact that the color vision of the foveal center is dichromatic, and that in his case a carefully fixated small field could be matched by a mixture of only two primaries. He further described the condition as similar to the uncommonly encountered variety of dichromasy known as tritanopia. Tritanopia is extremely rare, affecting an estimated 0.0001 per cent of the male population. In the past few years "small-subtense tritanopia" has been re-examined by Willmer (Ref. 12), Wright (Ref. 13), and Hartridge (Ref. 14). In general, the conclusion of Konig has been borne out, that the central fovea is indeed dichromatic and that the color confusions found with sufficiently small stimuli are consonant with the tritanopic pattern. Wright (Ref. 15) has recently measured the spectral sensitivity curves of seven tritanopes and has found them to be within the range of the spectral sensitivity curves of normal observers. Thus, there is no reason to expect that "small-subtense tritanopia" will have any marked influence on the spectral sensitivity curve of the central fovea obtained with small targets.

#### Purpose of the Present Study

From the foregoing analysis, it is apparent that the spectral sensitivity curve might well be expected to vary from point to point within the central fovea, depending upon the density of the macular pigment. Where the pigment is dense, the spectral sensitivity curve should be lowered over the considerable range of wavelengths absorbed to any appreciable extent by the macular pigment. The use of small test targets would be expected to maximize these differences, since with larger test objects there would undoubtedly be some sort of averaging process involved in the spectral sensitivity measure obtained. Presumably, spectral sensitivity variations from point to point would be related to the entoptic macular image. The spectral sensitivity should be reduced over the

short wave end of the spectrum whenever the entoptic macular image is dark, in comparison with the sensitivity in areas where the macular image is bright. The effect of the macular pigment should be maximal at 460  $\mu$ ; no effect would be expected for wavelengths longer than 570  $\mu$ .

Stiles (Ref. 16) provides data which add some support to this prediction. Stiles measured detection thresholds for a 10 minute test target at several locations within and outside the central fovea. The few data which were obtained demonstrate higher thresholds for the foveal area than for the immediately surrounding peripheral area for 435  $\mu$ , 475  $\mu$ , and 580  $\mu$  test targets. Thresholds for the foveal area lower than those for the immediately surrounding peripheral area were found for a 700  $\mu$  test target. These data show general agreement with the results to be expected from the known density of the macular pigment in these areas. The data for wavelengths 435 and 475  $\mu$  conform exactly to the expected effect of the macular pigment, as do the data for 700  $\mu$ . The data for 580  $\mu$  seem surprising if the macular pigment is indeed xanthophyll. Still, other factors such as photoreceptor density might be involved which would complicate interpretation of the results. This interpretation of the data would be greatly facilitated by having entire sensitivity curves for each retinal location studied.

The "small-subtense tritanopia" mechanism would not be expected to modify the spectral sensitivity curves for small test targets since the spectral sensitivity data for tritanopes are essentially normal. However, Crozier's data shown in Figure 2 could result from the involvement of a collection of cones differing from the usual collection with regard to the number of cones of each type. From this point of view, we might expect to obtain irregular appearing spectral sensitivity curves whenever small targets are utilized. Furthermore, these curves might be expected to differ for different locations of the test target within the central fovea, since there is no reason to expect that cones of the various types are equally numerous at various retinal locations.

The present study was designed, therefore, to assess possible variations in the spectral sensitivity curves obtained at different locations within the human fovea and to relate these variations to the presumed density of macular pigment as revealed by the macular entoptic plot. Measurements were made with a circular test target with a 1 minute diameter to avoid averaging results from different areas of the retina. It was expected that irregular spectral sensitivity curves might well be obtained because of variations in the relative number of cones of the various types from point to point.

## II. PROCEDURES AND APPARATUS

The general requirements placed upon the procedures and apparatus utilized in this study may be listed as follows:

1. spectral purity of the stimulus, of a degree attainable only with a spectroscopic instrument;
2. control of stimulus position on the retina, involving a suitably precise system of fixation and reasonably brief exposures;
3. control of stimulus size, by reduction of accommodative error and chromatic aberration of the eye; and
4. an adequate psychophysical method.

The procedures and apparatus utilized in the study are described in detail in the following sections.

### A. Observers

Three observers were used in the experiment: a color-normal male emmetrope (JHT), a color-normal female with corrected low-degree spherical and astigmatic errors (NLT), and a deuteranopic male emmetrope (DWM). Despite the considerable tedium of long and frequent observing sessions, motivation seemed to be sustained in all three observers during the entire course of the experiment. All three were highly trained in the specific observing task, and since the present study followed closely upon another experiment of rather similar nature in which two of the observers had served, practice effects were negligible.

### B. Stimulus Wavelengths

Initially, eleven wavelengths were chosen at approximately equal intervals throughout the visible spectrum. The exact wavelengths were chosen to match the dominant wavelength of interference filters used for fixation lights, as described below. As is well known, these filters must be coupled with suitable cut-off filters in order to eliminate secondary transmission peaks and the stray light resulting from the failure of the transmission to go to zero at intervening wavelengths. While the physical transmissions of these filter combinations indicate reasonable purity, the spectrophotometric curves alone are deceptive in terms of their visual effect at the ends of the spectrum. In order to arrive at the true visual peak wavelength it is essential to convert the physical measurements as follows: The spectrophotometric curves were first multiplied by the energy curve for tungsten at the appropriate color temperature utilizing the data of Skogland (Ref. 17). Then, the resultant values were multiplied by the visibility curve of the eye according to the values of Hardy (Ref. 18). The resultant curves of "visual effect" were plotted and the effective peak wavelengths were determined by use of a plane polar planimeter to locate the half-area

point on the wavelength abscissae. Wavelength values used hereafter in this report were specified in this way. The test target wavelengths were set to match the fixation lights and it was found that the values read from the wavelength drum of the monochromator agreed with the values computed in the manner described above. After the threshold data were collected with the initial set of eleven wavelengths, it became apparent that additional stimulus values were required in order to define the spectral sensitivity curves adequately in certain regions. Four additional wavelengths were selected for study on this basis. Thus, a total of fifteen different wavelengths were used in all.

### C. Foveal Location

In accordance with our intention of relating the spectral sensitivity curves to the entoptic macular images, three foveal locations were selected to represent different areas in the entoptic macular images reported by Miles (op. cit.). The first location, designated zero eccentricity, corresponded to the fixation point and hence to the center of the entoptic plot in all cases. This location presumably falls within the dark central area of the entoptic macular image described by Miles, corresponding to a pigmented area. The second location was at a point 15 minutes to the nasal side of center. This location was intended to fall within the intermediary bright annular band of the entoptic macular image described by Miles, corresponding to a pigment-free area. The third location was at a point 43 minutes to the nasal side of center. This location was intended to fall within the outermost dark annular area of the entoptic macular image described by Miles, corresponding again to a pigmented area. Actually, as will be discussed below, the macular entoptic images of all our observers did not conform to the classical pattern reported by Miles but these locations still represented meaningful differences in the macular images.

### D. Psychophysical Method

The advantages of the temporal forced-choice method of constant stimuli have been described in detail by Blackwell (Ref. 19), who has shown the superior validity and reliability obtained with this method. With this method, the observers have to correctly identify the interval, of four possible intervals, in which the target was presented. Five target intensities are utilized during an experimental session which yield probabilities of correct identification from little more than chance (.25) to nearly unity. A session consists of fifty presentations of each of the five target intensities. The intensities are presented in blocks of ten each of a given intensity, with the blocks of different intensity randomized in their order from session to session.

The probabilities of correct identification are corrected for chance successes from the relation

$$p' = \frac{p - .25}{1 - .25}$$

where  $p'$  = corrected probability; and  $p$  = raw probability.

Fortunately, these laboratories had available the necessary specialized equipment to utilize this method with convenience for the present study. Automatic stimulus presentation and recording equipment were utilized, which have been described elsewhere by Blackwell, Pritchard, and Ohmart (Ref. 20).

The psychophysical data obtained with this method represent values of corrected probability,  $p'$ , for each of five target intensities. These data were analyzed by a variant of the probit analysis reported elsewhere by Kincaid and Blackwell (Ref. 20). The analysis fits a normal ogive to the experimental data to satisfy the maximum likelihood criterion. The analysis method yields values of the intensity required for  $p' = .50$ , which is designated the threshold intensity. The analysis also provides a measure of the slope of the ogive, and measures of the standard errors of the threshold and the slope as well as a test for goodness of fit of the data to the normal ogive.

#### E. Other General Methodological Considerations

The use of an artificial pupil before the eye is mandatory in order to preclude differences in flux reaching the retina because of variations in the diameter of the natural pupil. In the present case a 6.04 mm. pupil was used, representing the maximum size believed safe under the conditions of the experiment.

The desirability of using fixation lights which match the stimulus in wavelength is self-evident. Reference to the published chromatic aberration curves for the human eye (for example Ref. 24) shows that use of, say, a red fixation point can result in the stimulus spot being as much as 3 diopters out of focus in the violet. This degree of blurring is exceedingly serious for the case of small stimuli, and intolerable in the present investigation which attempts to use targets whose angular size approaches the limits of the diffraction pattern. Additional precautions against chromatic error were taken by measuring and correcting for the chromatic aberration of each observer, as described below.

#### F. Plotting of the Entoptic Macular Image

We were fortunate to have obtained from Dr. Walter R. Miles then of Yale University samples of the filters used by him in the study already cited. The observers were seated before a light box which was masked down so that a bright patch of high color temperature white light subtending about 11 degrees was viewed through an aperture in a brow rest which controlled the eye-to-screen distance. A small fixation point was marked in the center of the bright area, and a piece of tracing paper affixed to the surface with tape. The observer was then required to practice alternating the pair of a chromatic and a neutral filter in front of his right eye until the entoptic macular image was seen and could be reproduced at will. Either of two different sets of filters supplied by Dr. Miles could be used by the observers, the only criterion

being maximization of the macular image. After a period of practice, each observer made a pencil sketch of the image directly on the tracing paper so that its angular size could subsequently be determined. The procedure was repeated at a later time to check the consistency of the result, essentially identical plots being obtained. One observer only (JHT) showed the three areas reported by Miles. A second (DWM) showed the three areas, but there appeared ray-like projection of the central area in both directions on the horizontal axis which extended well into the bright annular area. The remaining observer (NLT) showed no differentiation of the three areas, but sketched a more or less uniform dark spot which was slightly more dense at the center. The detailed discussion of these plots, together with their angular relationships is deferred until a later section.

#### G. Threshold Measurements

Threshold measurements were made with the psychophysical method described above. In a control room remote from the locus of observation an array of devices was located, whose function it was to send appropriate electrical signals to the point where the observing was done, to receive return signals indicating the responses made by the observer, and, after verifying the proper behavior of all phases of the presentation, to record the information relevant to all these on a record card. A tape-reader device and its associated relay panel cause the presentation of stimuli according to a sequence which provides trial-to-trial randomization of correct answers (i.e., any one of the four temporal intervals) as well as stimulus intensity randomization between five values but with these held constant for ten presentations at each intensity. Fifty single presentations constituted a single record card; five cards comprised an experimental session. An accessory counting device recorded the number of correct responses made to each of the five stimulus intensities.

The geometry of the observing station is diagrammed in Figure 3. The ribbon filament of the tungsten lamp is imaged at unity magnification on the entrance slit of the monochromator by means of a lens which is stopped down to an effective aperture of  $f. 4.4$  to avoid introduction of stray light into the monochromator. Attenuation of the beam is accomplished by the interposition of Wratten "neutral density" filters of fixed values, as well as by similar filters in the filter wheel which are alternately placed in the optical path in accordance with the appropriate electrical impulses from the remote automatic equipment. Between the lens and the slit, at a point of small focus, are two shutters. The first of these is a rotating sector driven by a Telechron motor in synchrony with the remote tape reader which allows passage of the beam for 0.1 second per revolution. The second shutter is a flag which is removed from the optical path only on signal from the remote scheduling equipment, and for a brief period which will let through only a single 0.1 second pulse.



The monochromator is a Hilger model D-246 with glass prism; the aperture ratio is  $f. 4.4$ . Calibration against the lines of mercury and sodium was carried out at the outset of the experiment and checked at the conclusion with sodium. No change in calibration occurred. The settings of the wavelength scale may be presumed accurate to 1 millimicron in the violet, and to 3 millimicrons in the red. Entrance and exit slits were maintained at .225 millimeters throughout the experiment, although the exit slit was stopped down by a tiny circular aperture subtending 1 minute of arc at the eye position, 750 mm. from the exit slit.

Fixation lights were introduced by reflection from a separate system, essentially a high-brightness lamp-house which produced the parallel light necessary for proper use of the interference filters. In every case, the brightness of the fixation lights was adjusted by the use of neutral filters to a comfortable level (approximately ten times threshold). A perforated mirror allowed unimpeded passage of rays from the monochromator to the eye, while accomplishing the introduction of the fixation cross images. Distance from the mirror to the exit slit was identical with distance from the mirror to the fixation lights. The mirror, a first-surface aluminized circle, was mounted on a nicely machined table which permitted rotation around a central vertical axis. By this means the eccentricity of the stimulus could be controlled by moving the reflected image of the fixation crosses in apparent space. A small projection system cast an image of a small incandescent filament onto a scale mounted on one wall of the observing room. Since part of the path of the projected image involved reflection of the rays from the mirror just mentioned, it was possible to calibrate the 0, 15 and 43 minute positions with considerable accuracy by the mirror's rotation of the beam.

At the eye of the observer a stray light shield was mounted and provision made for the introduction of ophthalmic correcting lenses and the artificial pupil. Proper alignment of all components was maintained by the use of rigid 'bite boards' bearing previously made molds of the complete dentition of the observers, in dental impression compound.

#### H. Radiometric Measurements

Total energy emergent at the exit slit of the monochromator at each of the initial wavelengths was measured by means of a thermopile so placed that all rays from the instrument fell within the limits of the blackened receiver. The associated electrical circuit is shown schematically in Figure 4 which indicates also the galvanometer, microammeter, shunt, variable resistances, switch and source of potential. It may be seen from this figure that the galvanometer is used merely as a sensitive null instrument, and that no dependence upon its absolute sensitivity calibration is necessary. Briefly stated, the radiometric procedure consists in adjustment of the bucking potential in the right arm of the circuit to a value which will just balance the e.m.f. produced by the thermopile. The current which will exactly nullify the thermoelectric potential will, of course, return the galvanometer coil to zero deflection, and its magnitude may be read directly in

microamperes. The thermopile was calibrated at the outset against a standard lamp, care being exercised to employ the identical circuitry to be used for the subsequent measurements. In the present case, it was determined that the thermopile generated one microvolt of potential for each 7.34 microwatts of energy incident upon its surface.

Owing to the relative insensitivity of the thermopile, it was necessary to make some compromise with spectral purity for the energy measurements. At atmospheric pressure our thermopile required the use of slit widths as great as 1 mm. at the shortest wavelength, although in the extreme red sufficient microammeter deflection could be obtained using 0.225 mm. slits. Fortunately the energy distribution of tungsten is such that the widest slits were necessary at those wavelengths where dispersion of the prism is greatest, and hence purity of the beam was not seriously affected.

Energy values determined by this method refer to total monochromator output at a variety of slit widths. Three further conversions are necessary before these values can be restated in terms of energy incident upon the cornea of the observer. First it is necessary to transform all values into terms of equal slit width, in the present case bringing them to 0.225 mm., a safe minimum value to preclude obstruction of the stimulus aperture. This slit width conversion was accomplished empirically by using the 931 photomultiplier photometer with the photocathode of the multiplier tube clamped rigidly in the position to be occupied by the observer's eye. Reduction factors from wide to narrow slits were determined from the ratio of narrow-slit to wide-slit readings at each wavelength. At this point the assumption is made that photocell response will change linearly as a function of flux reduction even though this reduction is accomplished in a manner that inevitably modifies the purity. Inspection of the published spectral sensitivity curve of the photomultiplier tube (Ref. 21) shows its maximum slope to be such that even our most extreme purity change resulting from slit width reduction amounts to only 3.8  $m\mu$  half width, and the average change to be a mere 1.2  $m\mu$ . This fact, together with the fact that the monochromator is equipped with symmetrically closing slits so that the center of that minute section of the photocell sensitivity curve important for the wavelength interval in question is approached as the slit jaws are closed, suggests that the assumption of linearity of photocell response is justified.

Having applied the slit width conversion factors to the original radiometric data to obtain energy values at uniform slit width, it now becomes necessary to reduce these values (which were measured using full-length slits) in accordance with the physical flux reduction imposed by the circular 1° stimulus aperture. For this purpose the photoelectric photometer was again used. A reduction factor was determined from the ratio of readings with and without the limiting aperture. (It should be mentioned parenthetically at this point that considerable care was taken to center the aperture over the exit slit of the monochromator.

This was done with the help of the photocell; its maximum response indicating optimal centering. Once achieved, this center position was rigidly maintained throughout the experiment.) By this technique, measuring at  $499.0 \text{ m}\mu$ , the factor converting energy at  $.225 \text{ mm. full-length slits}$  to the 1 minute circular aperture was found to be  $4.85 \times 10^{-3}$ .

Up to this point in the radiometric procedure we have found values to express total flux passing through the 1 minute aperture. The final conversion required to obtain the quantity of energy reaching the eye is based simply upon the geometric optics of the system. From a knowledge of the slit-to-eye distance and of the angle at which the rays from the slit diverge, one can readily compute the proportion of the total flux passing through an artificial pupil of known size, and hence accessible to the eye. In the present case, since the monochromator has an effective aperture of  $f. 4.4$ , the emergent cone of light has a half-angle of  $6.48$  degrees and the whole cone illuminates therefore an approximately circular area of  $228$  square centimeters. At the center of this round area is placed the artificial pupil whose diameter is  $.604$  centimeters and whose area is  $.286$  square centimeters. Strictly speaking, a direct areal conversion using these values is inadmissible owing to the cosine law of illumination. This law, which is commonly stated in the form:

$$E = \frac{I}{D^2} \cos \theta$$

expresses the fact that the circular patch is not uniformly bright, but rather that the peripheral illumination is always less than that on the axis of the cone. In the present instance, however, the peripheral value is within about a third of a percent of the axial one, and the inaccuracy introduced by assuming uniformity of flux across the area is inconsequential. This final reduction factor which permits computation of amounts of flux passing through the artificial pupil was found to be  $1.26 \times 10^{-3}$ .

Table I shows the results of the radiometric measurements. For each of the eleven wavelengths, the following information is given: the slit width necessary for suitable galvanometer response, monochromator output in microwatts at  $.225 \text{ mm. slits}$ , amount of energy at the eye, and an estimate of spectral purity. It should be stated that the half-width purity figures are derived from a crude empirical curve of dispersion, and represent only an approximation to the true values.

As indicated above, after collecting threshold data with these eleven wavelengths, it was considered desirable to study four additional wavelengths to assist in the definition of the spectral sensitivity curves. Radiometric measurements were not made for these wavelengths. Instead, radiometric values were estimated from smoothed curves relating radiant output to wavelength for the wavelengths actually measured. Since actual data points existed within less than  $15 \text{ m}\mu$  on either side of each of these four wavelengths, it is considered that this procedure cannot result in errors of appreciable magnitude.

### I. Chromatic Aberration Measurement

The oculometer, an instrument of outstanding usefulness in measuring the refractive condition of the eye under normal conditions of accommodation, has been described elsewhere by Ogle (Ref. 22). The observer looks through the artificial pupil at fixation crosses exactly as in the main part of the experiment, but with the single difference that the test target is replaced by the reflected image of a bright stigma seen reflected in the half-silvered mirror. Thus the eye simultaneously sees the fixation crosses at 750 mm. in real space as well as a point of light in the optical space created by the mirror and field lens. The lamp-house assembly, which carries the stigma, may be moved along the optic axis by the observer, changing the position of the bright point in apparent space. Now if the focal length of the field lens is known, the distance from it to the eye may be made equal to this focal length, and a linear scale may be affixed which can be calibrated directly in diopters. The scale modulus is determined from the dioptric strength of the field lens, and its zero point occurs where the stigma-to-lens distance is equal to the focal length of the lens and the image is at infinity.

In use, the observer views the two fixation crosses through the mirror and the reflected image of the stigma adjusted to appear between them. To obviate the possibility of using the stigma rather than the fixation crosses as an accommodative cue, the oculometer lamp is flashed continuously during the adjustments. Maintaining careful fixation, the job of the observer is to adjust the position of the stigma so that it appears in best focus. At this point the index of the oculometer scale will show the extent of accommodation in diopters. The average of a number of such settings is taken to represent the refractive state of the eye. As ordinarily used for the measurement of spherical error, the stigma as well as the external fixation device are illuminated by white light. Under these conditions the average scale reading is compared with the normal dioptric accommodation at a given distance and the discrepancy taken as indicative of spherical refractive error.

If, however, white fixation crosses are used in conjunction with chromatic stigmata, the instrument is converted into a sensitive device for the measurement of chromatic aberration. The observer adjusts the position of the stigma for best focus as before, but now the readings will deviate from the corresponding white-against-white ones by amounts depending upon the chromatic aberration curve of the eye. This system was used in the present study.

Approximately monochromatic stigmata were produced by the insertion of interference filters, together with their appropriate cut-off filters, between the oculometer lamp and the stigma. Brightnesses of the fixation crosses and stigma were adjusted for maximum ease of observation. Twenty settings of the oculometer were made by each observer at each of the eleven initial wavelengths under normal observing conditions (6.04 mm. artificial pupil and 750 mm. eye-to-object distance). Observers with

normal vision and free from persistent accommodative habits will tend to set the instrument at  $-1.33$  diopters, the theoretical normal refractive state for a viewing distance of  $750$  mm. Two observers (DWM and JHT) were approximately normal emmetropes, and their readings were therefore closely clustered about  $-1.33$  diopters in the yellow-green. The third observer (NLT) displayed both spherical and astigmatic errors which had to be corrected by placing ophthalmic lenses ( $+0.62$  sphere and  $+1.00$  cylinder) just in front of the artificial pupil. (In this position, correcting lenses of relatively weak power have a negligible effect upon the oculometer readings, although rigorously considered there will be some shift of the zero point of the scale as well as disturbance of the modulus and linearity.)

Results of the chromatic aberration measurements are plotted in Figure 5. (Values on the ordinate can be converted into terms of refractive error at each wavelength by subtraction of  $-1.33$  diopters from the obtained readings.) It must be emphasized that these values represent the combined errors resulting from uncorrected spherical as well as chromatic errors. For our purposes this seeming contamination of the curves is of no concern since the subsequent corrections will aim at removal of all errors regardless of cause.

It was not possible to obtain interference filters with peak wavelengths corresponding to the four wavelengths added after data on the initial eleven wavelengths had been analyzed. In each case, the fixation lights of wavelength most nearly equal were used. In no case was there more than a  $15 \text{ m}\mu$  difference in wavelength between the test target and the fixation lights. It is of course possible to determine from the data in Figure 5 the magnitude of refractive error to be expected from such a wavelength difference. In no case was there as much as a  $0.1$  diopter refractive error introduced in this way.

#### J. Corrections for Chromatic Aberration

Having measured chromatic aberration, it is now possible to provide ophthalmic corrections, provided certain other aspects of the system are taken into account. Crudely, one might simply introduce lenses of powers corresponding to the deviation from  $-1.33$  diopters at every wavelength. A somewhat more elaborate procedure was followed in this study in view of the precision desired for later computations.

The first step in this procedure was to approximate the indicated ophthalmic prescription by introducing lenses before the eye. For this purpose the lenses comprising a conventional ophthalmic test kit were used; hence we were limited to approximate corrections which, in the worst case, might fail as much as  $\pm 0.0265$  diopters to meet the desired value. One further complication arose from the impossibility of placing the lenses at the usual distance before the eye, and the consequent change in effective power. The usual test lens is calibrated for a specific distance from the eye ( $13.75$  mm. from anterior pole of the cornea in the Tillyer system). Changes from the nominal dioptric values were made to allow for this in

2455-10-F

the placement of the ophthalmic corrections.

With approximate corrections in place, we repeated the oculometric measurements in reverse. That is to say, in place of white fixation lights and chromatic stigmata, the color of the fixation crosses was controlled with interference filters while the stigma remained white. In the absence of correcting lenses this technique may be expected to yield a chromatic aberration curve which is reciprocally related to the already obtained one. Assuming that perfect correction of chromatic error had been achieved by the use of lenses, the refractive state of the eye would be constant, since chromatic differences in focus would have been neutralized. In the present case, owing to our inability to achieve exact correction, we would expect residual refractive errors. Algebraically added to these errors are undoubtedly errors in refraction arising from accommodative habit; together with errors of measurement these deviations from perfect correction combine to yield what we have called the residual error. Table II presents the residual errors at each wavelength for each of the three observers, computed according to the formula:

$$R.E. = \Delta[C - (A + B' + D)]$$

where A is the mean oculometer scale reading with chromatic stigma, B' the mean reading with white stigma and correcting lens, C the corrected lens power in diopters,  $\Delta$  the correction for chromatic aberration of the oculometer lens, and D = 2.66 diopters. It is evident from these data that the maximum error occurs at 475  $\mu$  for observer JHT. Under this, the worst condition, the retinal image is blurred to a size of approximately 4 minutes of arc. This raises the question of how much this degree of blurring will increase the energy required for visual detection. It may be inferred from the facts of spatial summation that blurring of this magnitude will not influence the detection threshold greatly, since the energy required for detection does not vary as a function of retinal image size to a considerable extent within these limits. It would perhaps seem a simple matter to revise the ophthalmic corrections by a second approximation, to produce zero refractive error. Unfortunately, this is impossible owing to the accommodative habits of the observers, who seem simply to accommodate out the additional lens power and revert to about the same refractive error. This instance of observers failing to accommodate so as to insure adequate ocular focus is of interest per se. It presumably is related to the fact that with chromatic stimuli to accommodation, best focus represents an accommodative condition which differs from that usually associated with the ocular vergence required to maintain binocular fusion. Rather than accept an accommodation-vergence relation which departs from the one which the observers usually adopts, the chromatic stimulus is allowed to blur somewhat.

### III. RESULTS AND DISCUSSION

The psychophysical data, representing 24,750 observations, were subjected to the variant of the probit analysis described in Section II

2455-10-F

above. The original probit estimates of the thresholds were multiplied by the radiometric data and corrected for attenuation by the neutral filter used in each case. Owing to the selective transmission of our so-called "neutral" Wratten filters, it was necessary to apply corrections to their white-light transmission values for each different wavelength target separately. This correction was applied for each of the fixed filters as well as for the psychophysical filter. The corrections were based upon spectrophotometric data for each filter involved. These manipulations result in threshold values in terms of total energy incident on the cornea, within the area of the pupillary aperture. Sensitivity values are represented by the inverse of these values.

Sensitivity values are presented for each observer in Tables III, IV, and V for each of the retinal locations studied. In a number of instances, the values represent averages of two experimental sessions. The data are plotted in Figures 6-8 for observer NLT, Figures 9-11 for observer JHT, and Figures 12-14 for observer DWM. The scales used for these figures are identical with those used in presenting the Hsia and Graham data in Figure 1 and the Crozier data in Figure 2.

Consider first the data for observer NLT, a color-normal female with a rather undifferentiated entoptic macular image. Although there are not a great many data points, it seems obvious that the spectral sensitivity curves are markedly different in the three locations. The standard errors of the sensitivity measures are well represented by the size of the data points, so that the manifested differences are highly significant from a statistical point of view. The curve for zero eccentricity is the smoothest, the curve for 15 minute eccentricity is next most smooth, and the curve for 43 minute eccentricity is most "irregular". There is a suggestion of bimodality in the data for the 43 minute eccentricity, with peaks at 555 and about 510  $m\mu$ .

The data for observer JHT, the color-normal male with the classical entoptic macular image, are entirely different. The curve for 43 minute eccentricity is the smoothest, the curve for zero eccentricity next most smooth, and the curve for 15 minute eccentricity is most "irregular". There is a definite suggestion of bimodality in all three curves. The peaks at zero eccentricity occur at about 525 and 575  $m\mu$ ; those at 15 minutes eccentricity occur at about 480 and 540  $m\mu$ ; and those at 43 minutes eccentricity occur at about 460 and 555  $m\mu$ .

The data for observer DWM, the deuteranopic male with the nearly classical entoptic macular image, are still different. The curve for zero eccentricity seems to be bimodal as does the curve for 43 minutes eccentricity. All the curves appear to be smooth but this may well be due to the fact that there are comparatively few data points. The curves for zero and 43 minute eccentricity appear to be bimodal with peaks at about 550 and 610  $m\mu$  in each case. The curve for 15 minute eccentricity has a single peak at about 550  $m\mu$ .

2455-10-F

Apparently, the most that can be concluded from these results is that the spectral sensitivity curve for point-size targets is by no means the same for the two different color-normal eyes and the deuteranopic eye, nor is the same for different retinal locations in the same eye. Thus, the spectral sensitivity curve measured for small retinal areas is highly idiosyncratic and there seems to be no simple way to characterize it. It is true that insufficient data exist to define these curves with complete adequacy; thus, there could be small irregularities of the type shown by the Crozier data which would have been missed. However, the differences among the curves are extremely large as examination of Tables III, IV and V will reveal. There can be little doubt that these differences are real.

It seems reasonable to interpret the differences among the spectral sensitivity curves as the result of different numbers of cones of various types in the different retinal locations studied. From this point of view, the peaks in the various curves presumably represent various types of cones. Peaks occur at 460, 480, 510, 525, 540, 555, and 610  $m\mu$ . Thus, these considerations would suggest the existence of seven cone photo-receptor systems. These peaks do not agree at all well with the peaks shown in the Crozier data. Unquestionably further measurements are needed to provide additional data points to define these peaks.

As noted in Section II, it was our intent to evaluate the extent to which variations in the spectral sensitivity curves from point to point correspond to differentiations in the entoptic macular images reported by the various observers. The data in Figures 6-14 have been replotted in Figures 15, 16, and 17 to facilitate this evaluation. The graphs for different locations have been replotted so as to agree at 575  $m\mu$  by shifting the curves for zero and 15 minute eccentricity to match the curve for 43 minute eccentricity at that wavelength. Adjustment to agreement at this point was selected since there is no appreciable absorption of wavelengths this long or longer by the macular pigment. Let us examine the relations shown in these figures in relation to the characteristics of the entoptic macular images reported by these observers.

As noted in Section II, observer NLT reported an entoptic macular image in the positive phase consisting of a uniformly dark center and a somewhat less dark surrounding area. The central area of the greatest darkness had a radius of 32 minutes; the outer zone of lesser darkness had an outer radius of 61 minutes. The pigment interpretation of the macular image would predict that the sensitivity for the blue end of the spectrum would be equivalent for zero and 15 minutes eccentricity but would be higher for the 43 minute eccentricity. The data presented in Figure 15 agree with this prediction exactly.

The macular image for observer JHT in the positive phase consisted of a small dark area of radius 11 minutes, surrounded by a bright annulus extending out to a radius of 28 minutes, with an outermost dark annulus extending out to a radius of 82 minutes. The pigment interpretation of the macular image leads to the prediction that blue-wavelength



2455-10-F

sensitivity for zero and 43 minutes eccentricity will be the same whereas the sensitivity for the 15 minute eccentricity will be higher. The data presented in Figure 16 agree with this prediction also.

The macular image for observer DWM (a deuteranope) in the positive phase consisted of a central dark area of radius 12 minutes, a dark surrounding annulus of radius 33 minutes, surrounded by a dark annulus of radius 61 minutes. However, there was an extension of the central dark area out entirely through the bright annular area on both sides along a generally horizontal meridian. Thus, we would expect to find equal sensitivity in the blue wavelength for all retinal locations. The data presented in Figure 17 agree generally with this prediction, at least in comparison with the differences in sensitivity found for the other two observers.

These data certainly lend considerable support to the hypothesis that blue wavelength spectral sensitivity varies from point to point in agreement with the location of dark and bright zones in the entoptic macular image. Since there is no reason to believe that "small-subtense tritanopia" would affect the sensitivity curves, this correspondence supports the view that the macular image is produced by differences in pigment density rather than differences in receptor populations as Walls (Ref. 23) has suggested.

2455-10-F

REFERENCES

1. Hsia, Y. and Graham, C. H. "Spectral Sensitivity of the Cones in the Dark Adapted Human Eye". Proc. Nat. Acad. Sci., 38, 80-85 (1952)
2. Sperling, H. G. "Some Comparisons Among Spectral Sensitivity Data Obtained in Different Retinal Locations and with Two Sizes of Foveal Stimulus". Ph.D. Dissertation, Columbia University, Univ. Microfilms No. 6711, 23 p. (1953)
3. Crozier, W. J. "On the Visibility of Radiation at the Human Fovea". J. Gen. Physiol., 34, 87-136 (1950)
4. Polyak, S. The Retina. Chicago: Univ. Chicago Press, 607 p. (1941)
5. Buzzi, F. "Nuove sperienze fatte sull'occhio umano". In Opuscoli scelti sulle scienze e sulle arti, v. 5. Milano: G. Marelli (1782)
6. Gullstrand, A. "Die Farbe der Macula centralis retinae" v. Graefes Arch. Ophthal., 62, 378 (1905)
7. Maxwell, J. C. "On the Unequal Sensibility of the Foramen Centrale to Light of Different Colours". Athenaeum, No. 1505, 1093 (1856)
8. Helmholtz, H. von. Treatise on physiological optics. (Trans. J.P.C. Southall) v. 2, Menasha; Banta, (1924)
9. Miles, W. R. "Entopic Plotting of the Macular Area". Proc. Army-Navy-OSRD Vis. Comm., 14th meeting, 13-26 (1945)
10. Wald, G. "Human Vision and the Spectrum". Science, 101, 653-658 (1945)
11. König, A. In S. B. Akad. Wiss. Berl., 577 (1894)
12. Willmer, E. N. "Colour Vision in the Central Fovea". Documenta Ophthalmologica, 3, 194-213 (1949)
13. Wright, W. D. Researches on Normal and Defective Colour Vision. St. Louis: Moxby, 383 p. (1947)
14. Hartridge, H. "The Colour of Small Objects", J. Physiol., 104, 2 (1946)

2455-10-F

REFERENCES (cont'd)

15. Wright, W. D. "The Characteristics of Tritanopia". J. Opt. Soc. Amer., 42, 509-521 (1952)
16. Stiles, W. S. "Increment Thresholds and the Mechanisms of Colour Vision". Documenta ophthalmologica 3, 138-163 (1949)
17. Skogland, J. F. Tables of spectral energy distribution and relative brightness from spectrophotometric data. Washington: N.B.S. Miscellaneous publication 86, (1929)
18. Hardy, A. C. Handbook of Colorimetry. Cambridge: The Technology Press, 87 p. (1956)
19. Blackwell, H. R. Psychophysical Thresholds: Experimental Studies of Methods of Measurement. University of Michigan, Engineering Research Bulletin No. 36, 227 p. (1953)
20. Kincaid and Blackwell, "Application of Probit Analysis to Psychophysical Data. I. Techniques for Desk Computation". University of Michigan, Engineering Research Institute Report 2144-283-T (in press)
21. Zworykin, V. K. and Ramberg, E. G. Photoelectricity and Its Application. New York: Wiley (1949)
22. Ogle, K. N. Notes on the Stigmatoscopy Method of Refraction. Unpublished paper. 12 p. (1947)
23. Walls, G. L. and Mathews, R. W. "New Means of Studying Color Blindness and Normal Foveal Color Vision: With Some Results and Their Genetical Implications" Univ. of Calif. Publications in Psychol., 7, 1-172 (1952)
24. Wald, G. and Griffin, D. R. "The Change in Refractive Power of the Human Eye in Dim and Bright Light". J. Opt. Soc. Amer., 37, 321-336 (1947)

2455-10-F  
TABLE I

SUMMARY OF RADIOMETRIC MEASUREMENTS AND THEIR CONVERSION TO UNITS OF ENERGY AT THE CORNEA

Wavelength (m $\mu$ )	423.5	459.0	475.0	499.0	526.5	553.0	571.0	606.0	635.0	669.0	698.0
Slit Width (mm)	1.000	0.750	0.750	0.500	0.375	0.375	0.250	0.225	0.225	0.225	0.225
Microamperes with R <sub>e</sub> = 0.4 ohms.	1.89	2.87	4.04	2.90	2.51	3.80	2.06	3.08	3.28	4.29	5.13
Microvolts	0.756	1.15	1.62	1.16	1.00	1.52	0.824	1.23	1.31	1.72	2.05
Microwatts	5.55	8.44	11.89	8.51	7.34	11.16	6.05	9.03	9.62	12.60	15.04
Empirical Conversion to .225 mm. slit	.0393	.0682	.0871	.188	.357	.343	.830	.775	1.000	1.000	1.000
Microwatts with .225 mm. slit	.218	.576	1.036	1.600	2.62	3.83	5.02	7.00	9.62	12.60	15.04
Microwatts with 1 minute aperture	1.06 x 10 <sup>-3</sup>	2.79 x 10 <sup>-3</sup>	5.02 x 10 <sup>-3</sup>	7.76 x 10 <sup>-3</sup>	1.27 x 10 <sup>-2</sup>	1.86 x 10 <sup>-2</sup>	2.43 x 10 <sup>-2</sup>	3.49 x 10 <sup>-2</sup>	4.67 x 10 <sup>-2</sup>	6.11 x 10 <sup>-2</sup>	7.29 x 10 <sup>-2</sup>
Microwatts through 6.04 mm. pupil	1.34 x 10 <sup>-6</sup>	3.52 x 10 <sup>-6</sup>	6.33 x 10 <sup>-6</sup>	9.78 x 10 <sup>-6</sup>	1.60 x 10 <sup>-5</sup>	2.34 x 10 <sup>-5</sup>	3.06 x 10 <sup>-5</sup>	4.28 x 10 <sup>-5</sup>	5.88 x 10 <sup>-5</sup>	7.70 x 10 <sup>-5</sup>	9.19 x 10 <sup>-5</sup>
Estimated Half-width purity (m $\mu$ )	.3	1.3	1.7	2.3	2.7	3.3	3.7	4.5	2.5	3.0	3.5

TABLE II

RESIDUAL ERRORS AFTER CORRECTION FOR CHROMATIC ABERRATION (diopters)

Wavelength (mμ)	Observer		
	JHT	NLT	DWM
423.5	-.342	-.001	+.001
459.0	-.354	-.009	+.281
475.0	-.568	-.180	+.018
499.0	-.318	-.132	+.312
526.5	-.377	+.139	+.214
553.0	-.201	-.026	+.282
571.0	-.223	-.023	+.190
606.0	-.154	+.229	+.301
635.0	-.174	+.179	-.019
669.0	-.220	+.212	+.090
698.0	-.093	-.037	+.093

SPECTRAL SENSITIVITY FOR OBSERVER NLT;

Inverse Threshold Radiosity (microwatts  $\times 10^{-6}$ )

Wavelength ( $m\mu$ )	Eccentricity		
	0	15 minutes	43 minutes
423.5	$5.05 \times 10^6$	$6.33 \times 10^6$	$3.77 \times 10^6$
459.0	$1.20 \times 10^7$	$9.57 \times 10^6$	$2.39 \times 10^7$
475.0	$2.48 \times 10^7$	$2.67 \times 10^7$	$3.22 \times 10^7$
499.0	$6.41 \times 10^7$	$5.00 \times 10^7$	$8.93 \times 10^7$
514.0			$9.10 \times 10^7$
526.5	$2.05 \times 10^8$	$1.76 \times 10^8$	$1.09 \times 10^8$
540.0	$3.40 \times 10^8$	$3.12 \times 10^8$	$1.75 \times 10^8$
553.0	$3.56 \times 10^8$	$3.69 \times 10^8$	$2.68 \times 10^8$
571.0	$3.23 \times 10^8$	$2.78 \times 10^8$	$1.57 \times 10^8$
606.0	$2.16 \times 10^8$	$1.52 \times 10^8$	$1.00 \times 10^8$
635.0	$5.65 \times 10^7$	$4.88 \times 10^7$	$3.18 \times 10^7$
669.0	$8.93 \times 10^6$	$5.18 \times 10^6$	$7.63 \times 10^6$
698.0	$1.44 \times 10^6$	$9.80 \times 10^5$	$8.15 \times 10^5$

2455-10-F

TABLE IV

SPECTRAL SENSITIVITY FOR OBSERVER JHT

Inverse Threshold Radiosity (Microwatts  $\times 10^{-6}$ )

Wavelength ( $m\mu$ )	Eccentricity		
	0	15 minutes	43 minutes
423.5	$6.94 \times 10^6$	$7.04 \times 10^6$	$2.48 \times 10^6$
459.0	$1.34 \times 10^7$	$1.39 \times 10^7$	$9.09 \times 10^6$
467.0			$8.44 \times 10^6$
475.0	$2.14 \times 10^7$	$3.40 \times 10^7$	$8.70 \times 10^6$
487.0		$3.44 \times 10^7$	
499.0	$5.99 \times 10^7$	$4.27 \times 10^7$	$3.50 \times 10^7$
514.0			$5.74 \times 10^7$
526.5	$3.26 \times 10^8$	$1.50 \times 10^8$	$8.93 \times 10^7$
540.0	$2.87 \times 10^8$	$2.15 \times 10^8$	$1.17 \times 10^8$
553.0	$2.81 \times 10^8$	$1.07 \times 10^8$	$1.49 \times 10^8$
571.0	$3.88 \times 10^8$	$1.01 \times 10^8$	$1.51 \times 10^8$
606.0	$2.27 \times 10^8$	$5.52 \times 10^7$	$6.90 \times 10^7$
635.0	$1.70 \times 10^8$	$2.00 \times 10^7$	$1.45 \times 10^7$
669.0	$1.39 \times 10^7$	$7.14 \times 10^6$	$4.81 \times 10^6$
698.0	$2.04 \times 10^6$	$1.48 \times 10^6$	$5.21 \times 10^5$

SPECTRAL SENSITIVITY FOR OBSERVER DWM;  
Inverse Threshold Radiosity (microwatts  $\times 10^{-6}$ )

Wavelength ( $\mu$ )	Eccentricity		
	0	15 minutes	43 minutes
423.5	$8.93 \times 10^6$	$5.92 \times 10^6$	$7.58 \times 10^6$
459.0	$1.10 \times 10^7$	$1.08 \times 10^7$	$2.20 \times 10^7$
475.0	$2.05 \times 10^7$	$2.62 \times 10^7$	$2.19 \times 10^7$
499.0	$7.63 \times 10^7$	$3.88 \times 10^7$	$5.43 \times 10^7$
526.5	$3.11 \times 10^8$	$2.21 \times 10^8$	$1.64 \times 10^8$
553.0	$3.85 \times 10^8$	$3.51 \times 10^8$	$2.38 \times 10^8$
571.0	$3.03 \times 10^8$	$2.29 \times 10^8$	$1.82 \times 10^8$
606.0	$3.18 \times 10^8$	$1.58 \times 10^8$	$2.86 \times 10^8$
635.0	$2.54 \times 10^8$	$6.62 \times 10^7$	$4.72 \times 10^7$
669.0	$4.02 \times 10^7$	$1.34 \times 10^7$	$1.03 \times 10^7$
698.0	$2.42 \times 10^6$	$1.49 \times 10^6$	$9.26 \times 10^5$



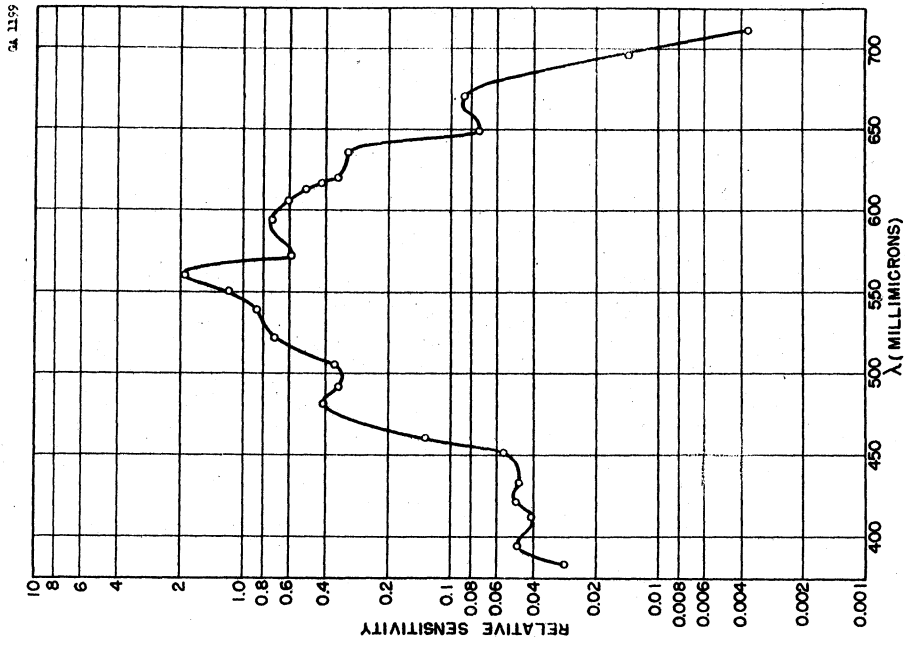


Fig. 2. Data of Crozier.

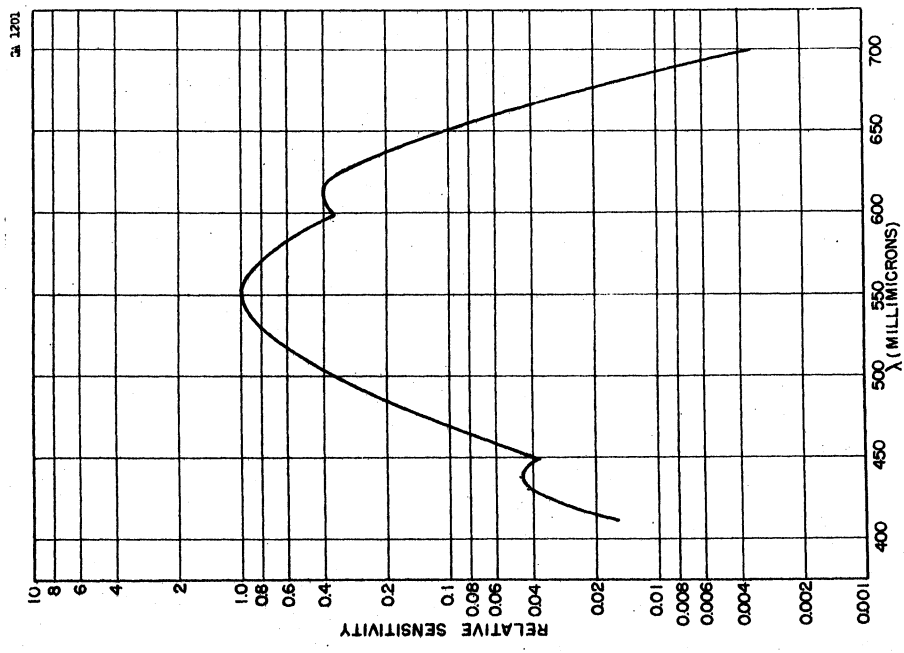


Fig. 1. Data of Hsia and Graham.

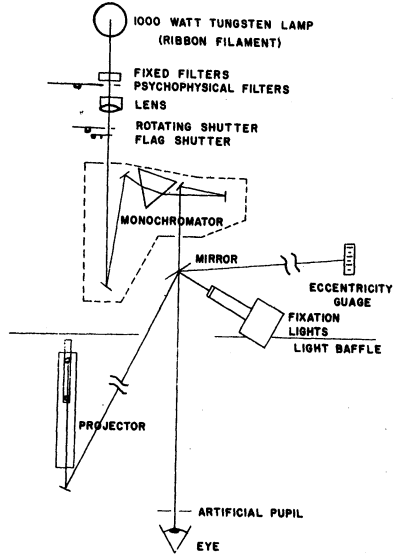


Fig. 3. Optical schematic drawing of the stimulus presentation equipment.

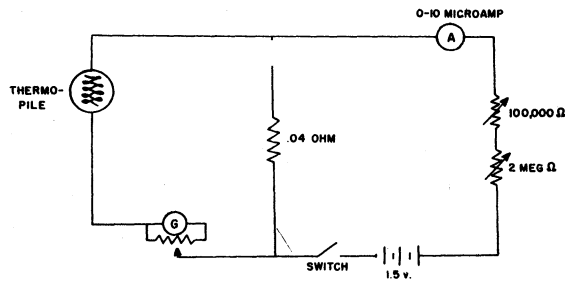


Fig. 4. Circuit for the radiometric equipment.

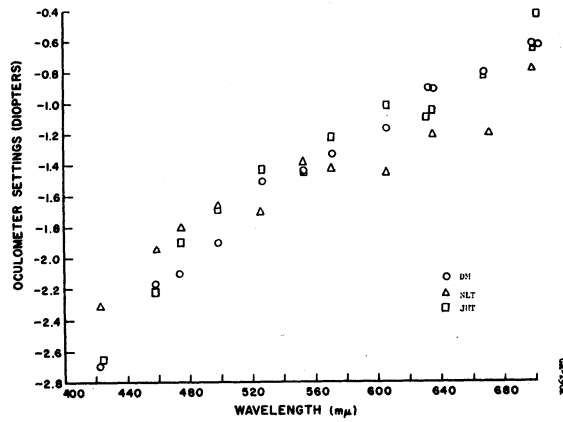


Fig. 5. Chromatic aberration measurements.

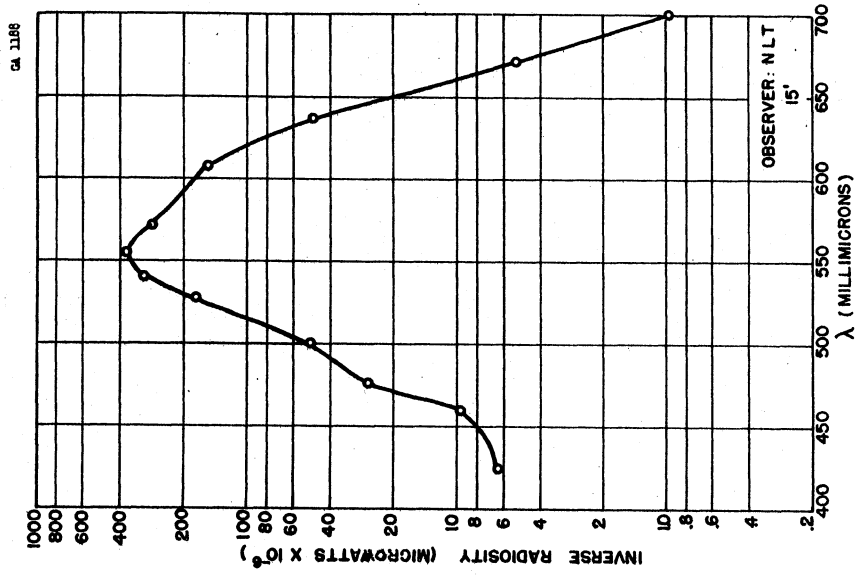


Fig. 7. Threshold data.

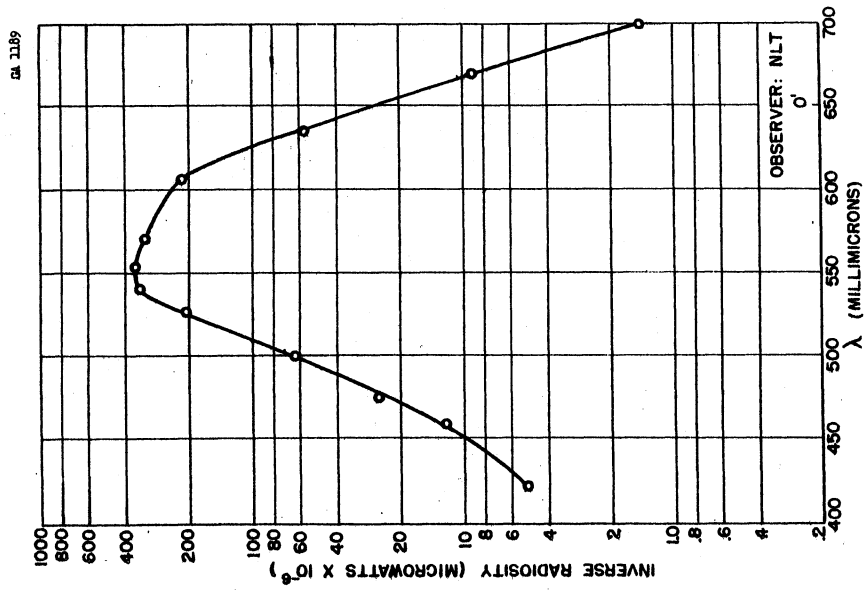


Fig. 6. Threshold data.

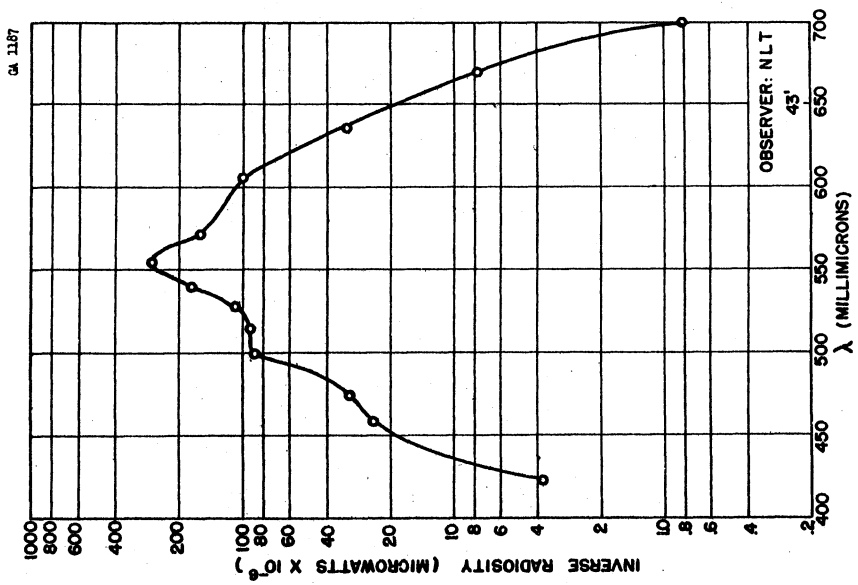


Fig. 8. Threshold data.

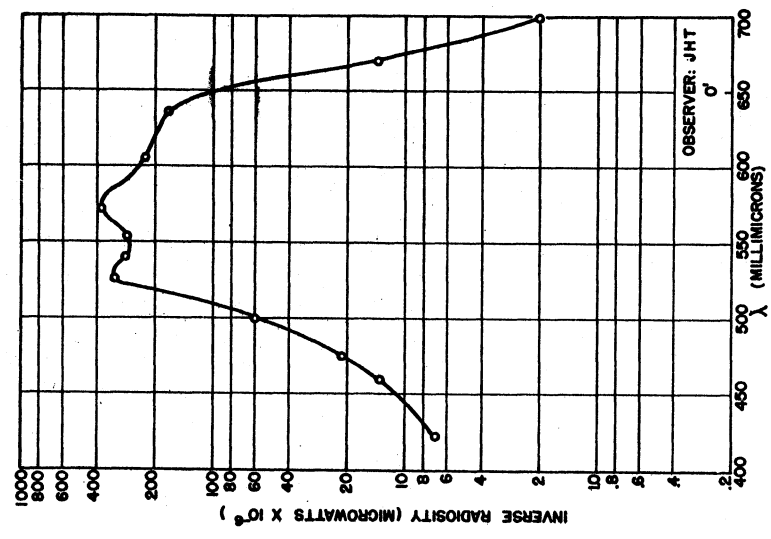


Fig. 9. Threshold data.

CA 1186

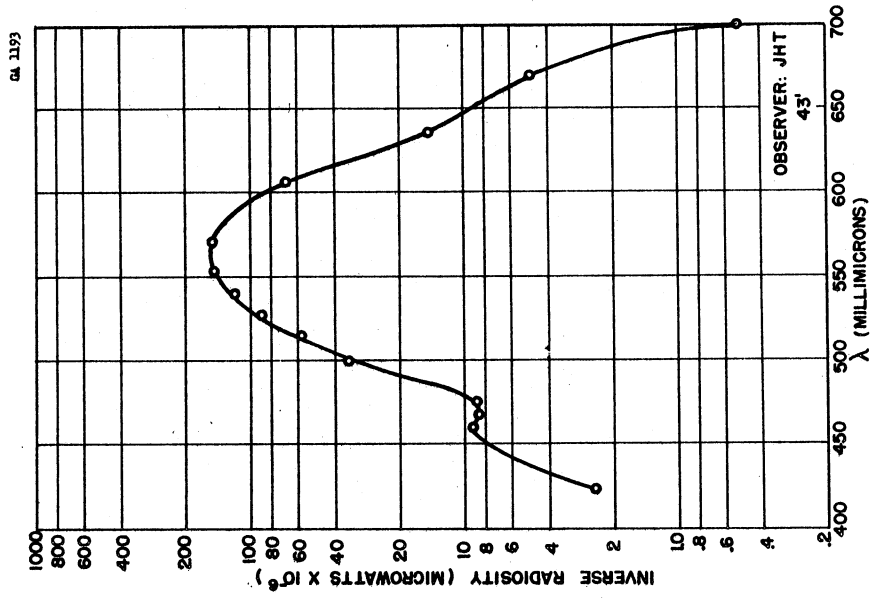


Fig. 11. Threshold data.

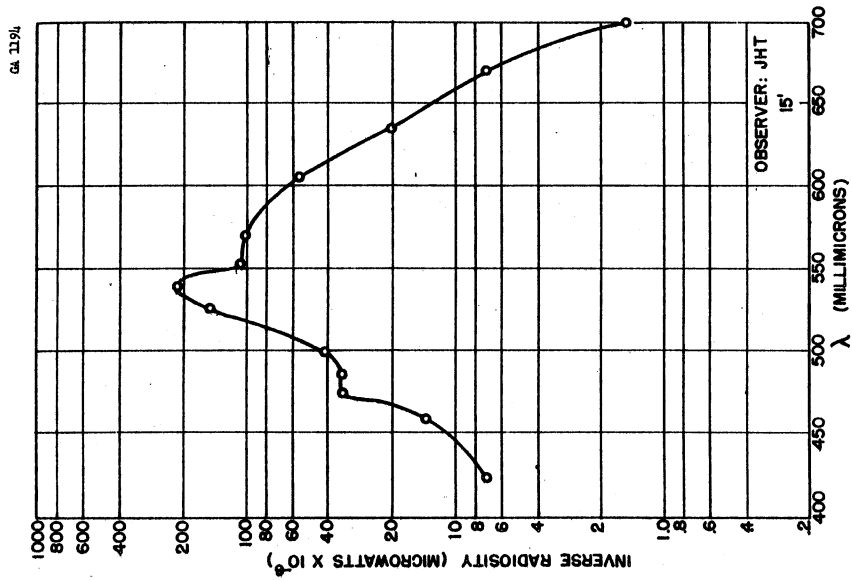


Fig. 10. Threshold data.

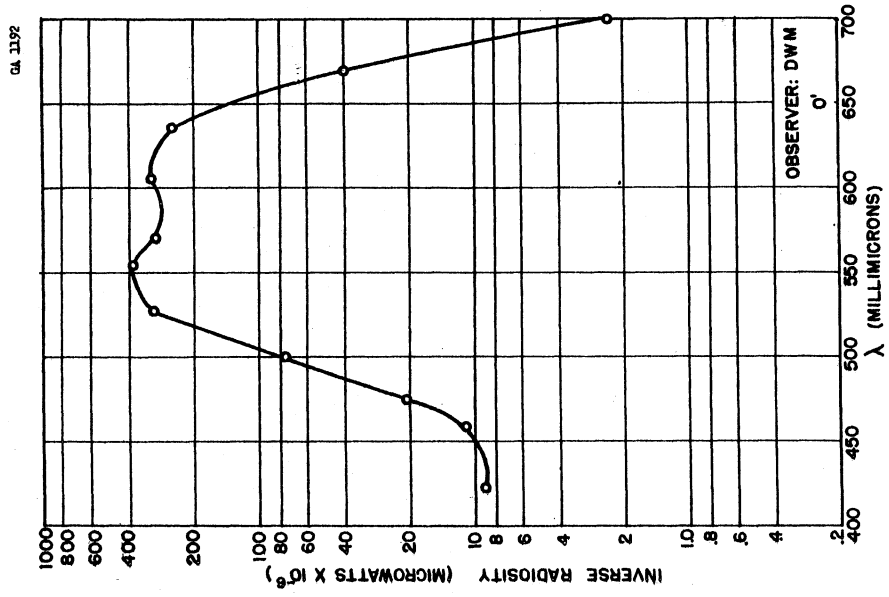


Fig. 12. Threshold data.

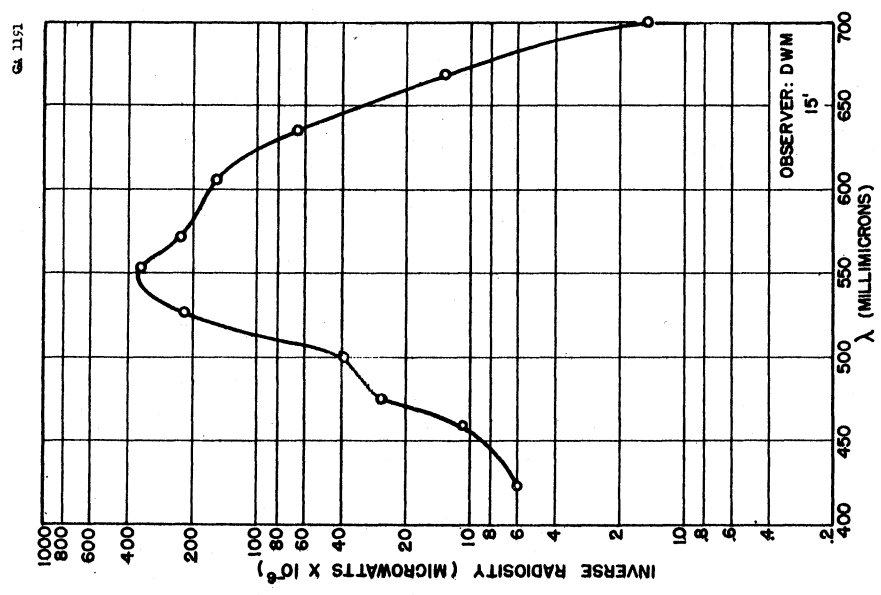


Fig. 13. Threshold data.

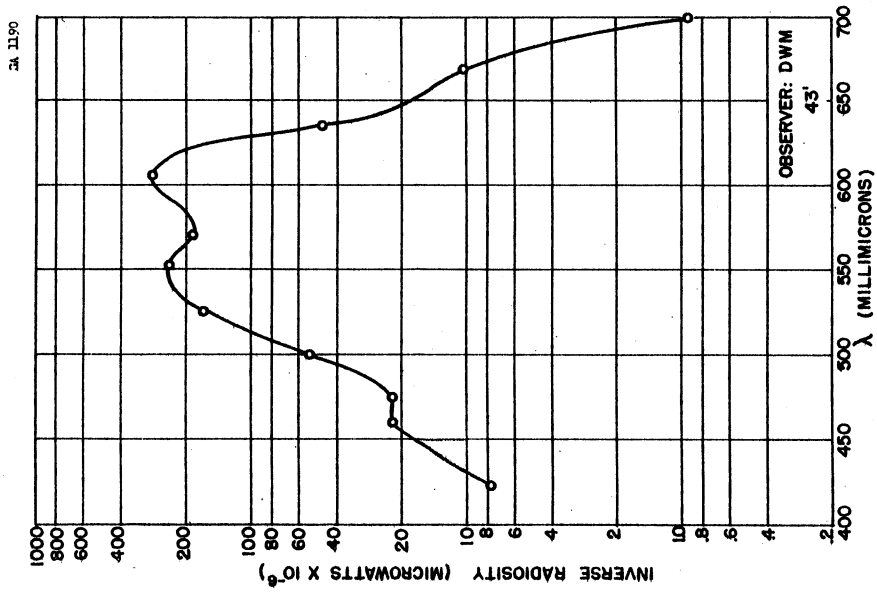


Fig. 14. Threshold data.

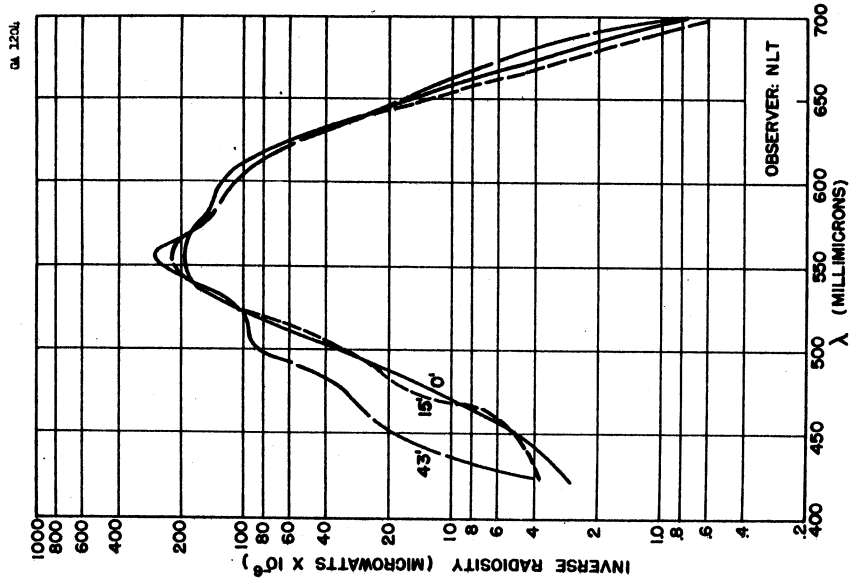


Fig. 15. Adjusted threshold data.

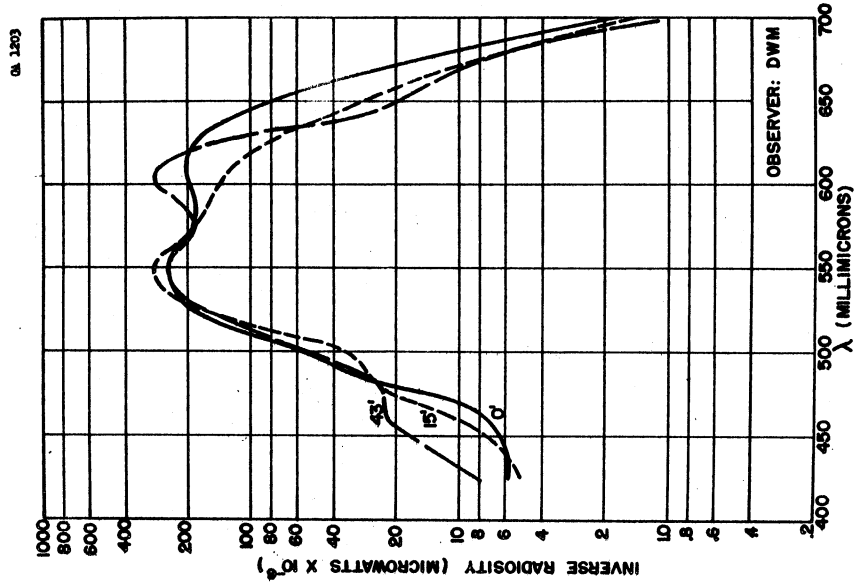


Fig. 17. Adjusted threshold data.

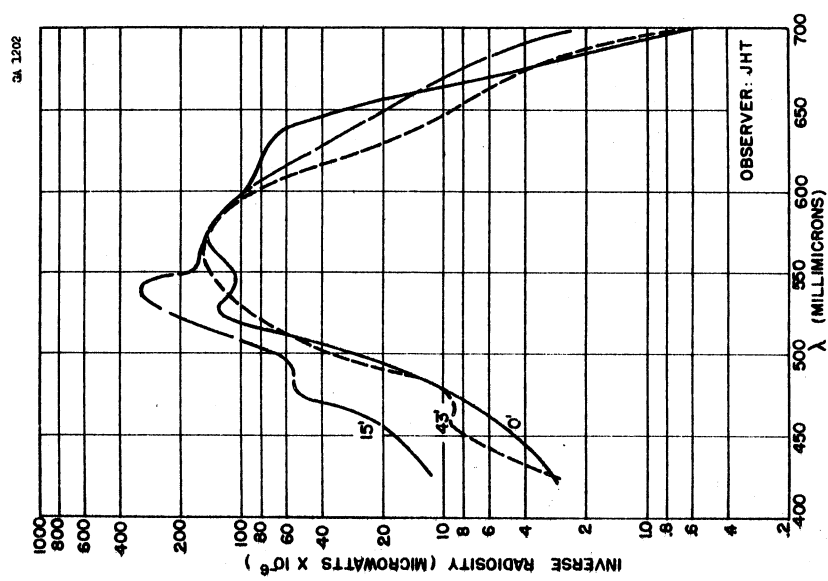


Fig. 16. Adjusted threshold data.



UNIVERSITY OF MICHIGAN



3 9015 02514 7854